WATER RESOURCES RESEARCH, VOL. 46, W07520, doi:10.1029/2009WR008835, 2010

Role of microtopography in rainfall-runoff partitioning: An analysis using idealized geometry

Sally E. Thompson,[1] Gabriel G. Katul,[1] and Amilcare Porporato[2]

Received 29 October 2009; revised 11 February 2010; accepted 24 February 2010; published 16 July 2010.

[1] Microtopography, consisting of small-scale excursions in the elevation of the land surface on millimeter to centimeter scales, is ubiquitous on hillslopes, but its effects are rarely incorporated into hydrological analyses of rainfall-runoff partitioning. To progress toward a hydrological theory that accounts for microtopography, two research questions are considered: (1) Does microtopography change the partitioning of rainfall into runoff and infiltration compared to a background case that lacks these small-scale excursions? and (2) how do soil, mean slope, storm properties, and microtopographic geometric attributes influence this partitioning? To address these questions, a simplified one-dimensional hillslope with uniform sinusoidal microtopography is considered, and several rainfall-runoff scenarios are examined with a numerical model. The results indicate that for a range of realistic conditions, microtopography increases the proportion of rainfall infiltrating by 20–200% relative to an equivalent "background state" in which microtopography is absent. Additional theoretical development addressing issues of connectivity and improved representations of flow hydraulics over microtopographic surfaces are needed to refine these estimates and extend them to less idealized conditions. If confirmed, the results suggest that microtopography may have a significant impact on streamflow generation, plant water availability and the co-evolution of geomorphic, hydrological and ecological systems, with important implications for land management, especially in arid ecosystems.

Citation: Thompson, S. E., G. G. Katul, and A. Porporato (2010), Role of microtopography in rainfall-runoff partitioning: An analysis using idealized geometry, *Water Resour. Res.*, *46*, W07520, doi:10.1029/2009WR008835.

1. Introduction

[2] The small-scale profile of surfaces, or their microtopography, is of interest across many diverse disciplines including microfluidics, metallurgy, biophysics, and materials science. It is particularly important in determining the interactions of a surface with other substances and its immediate environment [*Costa*, 2004; *Hale and Mitchell*, 2002; *Lloyd*, 2003; *Semler et al.*, 2006; *Vanenckevort*, 1984]. Microtopography is also important in the geosciences, where it refers to topographic variation about a mean surface trend with amplitudes much smaller than hillslope or basin scales.

[3] In arid and semi-arid environments, the partitioning of rainfall between infiltration and runoff at the soil surface is particularly important, since water lost to Hortonian runoff processes cannot contribute to sustaining vegetation at a site (although it may contribute to the growth of vegetation at sites downslope) [*Descroix et al.*, 2007; *Kirkby and Chorley*, 1967; *Lehmann et al.*, 2007; *Noy-Meir*, 1979]. Microtopography is anticipated to play an important role in ecohydrological processes of arid and semi-arid systems.

[4] Hydrologically, microtopography may be characterized by two distinguishing features: (1) the vertical variations are on the same order of magnitude as the flow depth during runoff events (i.e., mm to cm), and (2) the horizontal variation of the microtopographic features are 2–3 orders of magnitude smaller than the hillslope length (i.e., 10 to 100 cm). The geometric attributes of these features can be variable (Figure 1), and may be produced by biogenic or physical processes. The statistical and scaling properties of microtopography on natural hillslopes have rarely been quantified. Data from tillage research suggests that much of the natural variation of the soil surface is fractal [*Burrough*, 1983; *Pardini and Gallart*, 1998; *Perfect and Kay*, 1995; *Vazquez et al.*, 2005], while larger scales of topographic variation (i.e., 2–5 m scales associated with dunes and vegetation mounding) also display power law scaling [*Pachepsky and Ritchie*, 1998; *Pachepsky et al.*, 1997].

[5] Despite its ubiquity, microtopography is rarely incorporated into hydrological analyses except in the parameterization of roughness coefficients. The effects of microtopography have been investigated in tillage research, and largely considered the consequences of tillage on slowing runoff and erosion [*Allmaras et al.*, 1966; *de Lima et al.*, 1989; *Gayle and Skaggs*, 1978; *Hansen et al.*, 1999; *Linden and Vandoren*, 1986; *Mitchell and Jones*, 1976; *Mohamoud et al.*, 1990; *Onstad*, 1984; *Planchon et al.*, 2002; *Van Oost et al.*, 2006; *Zobeck and Onstad*, 1987]. The results have been equivocal: many studies indicate a reduction in erosion and runoff in the presence of increased

[1]Nicholas School of the Environment, Duke University, Durham, North Carolina, USA.
[2]Pratt School of Engineering, Duke University, Durham, North Carolina, USA.

0043-1397/10/2009WR008835

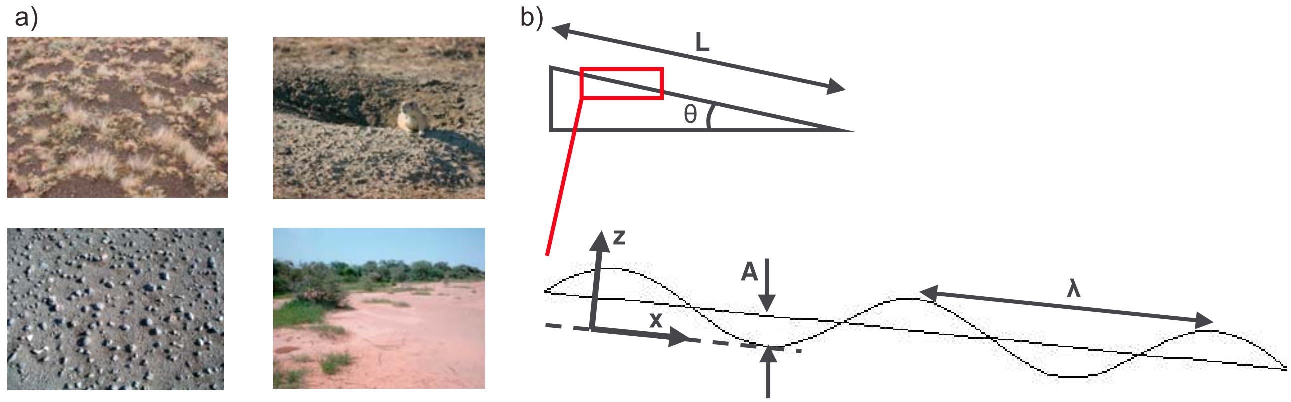

Figure 1. (a) Examples of microtopographic variation: (top left) terracette formation on hillslopes in Idaho (formed by interaction of vegetation, erosion and flow), (top right) prairie dog mounds (formed by fauna), (bottom left) stony desert pavement (formed by aeolian erosion), and (bottom right) mounding associated with vegetation in semi-arid woodlands (formed by aeolian and rain splash erosion). (b) Definition of geometric parameters describing the hillslope and microtopography. The top images in Figure 1a are courtesy of Ciaran Harman. The bottom left image in Figure 1a is from L. Deschodt (Desert pavement, 2003, available from Wikimedia Commons at http://commons.wikimedia.org/wiki/File:Desert_pavement_Myrdalssandur.JPG), and the bottom right image in Figure 1a is from M. Schmidt (Vegetation band in tiger bush near Zamarkoye, Burkina Faso, 2004, available from Wikinedia Commons at http://commons.wikimedia.org/wiki/File:Tigerbusch_Vegetationsband_Marco_Schmidt_0773.jpg).

microtopographic variation [*Johnson et al.*, 1979; *Steichen*, 1984], while other studies found that roughness increased erosion rates, presumably by concentrating the flow [*Darboux and Huang*, 2005; *Helming et al.*, 1998]. Microtopography has been investigated in the context of "interactive infiltration" studies, which explicitly account for variability in infiltration and runoff behavior when the two processes are coupled across a hillslope, resulting in "an areal hydrologic [runoff] response not typified by classical point-scale infiltration theory" [*Fiedler et al.*, 2002, p. 293]. A few studies have shown significant perturbations in infiltration and runoff response when surface elevation variation is accounted for, compared to microtopographically smooth surfaces [*Fiedler et al.*, 2002; *Tayfur et al.*, 1993].

[6] The governing equations that may be used to describe hillslope hydrology are the shallow water equations for surface runoff flow and Richards' equation for infiltration and soil moisture redistribution. Accounting for microtopography requires that these equations be coupled across all spatially variable boundaries. This coupling problem was confronted via brute-force numerical simulations [*Esteves et al.*, 2000; *Fiedler and Ramirez*, 2000; *Tayfur et al.*, 1993], but such approach has several drawbacks. First, the spatial scales that must be resolved span the finest microtopographic detail to the entire hillslope length. Similar scale issues arise in the temporal domain, with scales ranging from seconds-minutes for the activation of overland flow, to several months over which subsurface redistribution determines soil moisture conditions. This high dimensionality in space and time, coupled with the need for high-resolution characterization of the microtopography and soil properties as well as site specific calibration [*Esteves et al.*, 2000; *Fiedler and Ramirez*, 2000; *Tayfur et al.*, 1993], prohibits a general treatment of microtopography through direct simulations of the governing equations and indeed the effects of microtopography on hydrological response have largely resisted a generalizable theoretical treatment. An exception is a study by *Dunne et al.* [1991] that considered the effects of tillage-like microtopography where flow occurred in channels between "hills." Dunne et al. showed how correlations between the height of these features and their infiltration capacity resulted in a nonlinear scaling of hillslope-scale infiltration capacity with the depth of flow.

[7] Here, "first-order" effects of microtopography on runoff-infiltration partitioning for simplified cases are analyzed. Our goal is to provide a complementary approach to that adopted by *Dunne et al.* [1991] in complexity and ease of making generalizations. Given the focus on arid and semi-arid environments we target at the storm event scale and treat storm events as essentially independent.

2. Conceptual View

[8] Consider a sloping surface with microtopographic variability consisting of mounds and depressions of different sizes. If this surface is exposed to persistent rainfall, and rainfall intensity ($I(t)$) exceeds the infiltration capacity ($f(t)$), then a number of different regimes can be defined (Figure 2) [*Horton*, 1945]. Prior to ponding, water infiltrates without surface redistribution. Following surface ponding, ponded water collects in depressions, delaying the onset of runoff from the immediate catchment of each depression (case A). As the smallest depressions overtop, runoff establishes flow and hydrologic connectivity between upslope and downslope locations (case B). Eventually, this connectivity links runoff flow paths to the channel, allowing export of surface water from the hillslope. As the depth of flow on the surface increases, some of the microtopographic features are submerged, creating a complex 2–3 dimensional "mixed flow" regime around emergent microtopographic mounds (case C).

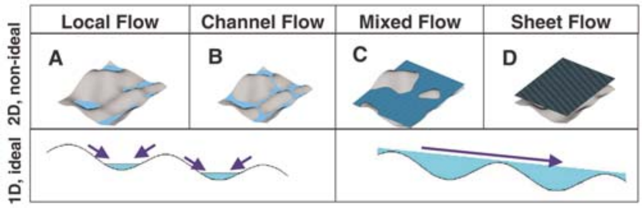

Figure 2. Separation of the storm event into multiple flow regimes depending on the degree of inundation of the microtopographic features. Our focus here is on the "end-member" cases A and D.

Further increases in water depth "drown" these features, leading to a sheet flow condition (case D).

[9] Conceptualizing these cases separately allows for different simplifications to be made to the governing equations. Replacing a "real" microtopographic surface with an idealized version permits further simplifications. For instance, on an idealized one-dimensional hillslope with uniform sinusoidal microtopography, cases B and C do not occur since depressions fill and over-top uniformly, immediately generating sheet flow (case D). In such an ideal case, a "toy model" describing rainfall-runoff partitioning requires only three components: a model of the surface prior to ponding, the filling of the surface store as described in case A and sheet flow over the microtopography as described in case D. Although simple, this sinusoidal microtopography offers some key advantages. First, any general theory for complex microtopography, must, in the limit, recover this idealized set up. Second, the orientation of microtopography here is at 90° to that utilized in the study by *Dunne et al.* [1991], allowing the two cases to be considered as "end-members" that constrain plausible flow behavior on microtopographically varying landscapes. Finally, a large number of studies already consider the problem of how a wavy surface affects bulk flow properties [*Poggi et al.*, 2007]. Hence, this representation of microtopography allows us to draw from a rich literature in fluid mechanics when describing flow responses [*Belcher and Hunt*, 1993, 1998; *Finnigan and Belcher*, 2004; *Patton and Katul*, 2009; *Poggi et al.*, 2008]. In short, a sinusoidal topography provides a parsimonious and tractable representation of the variable surface and its effects on infiltration and surface runoff.

3. Idealized Model and Assumptions

[10] As outlined above, the idealized model consists of a 1-D hillslope on which microtopographic variation is represented as sinusoidal excursions with fixed amplitude A and fixed wavelength λ as shown in Figure 1b. Soil properties, specifically the hydraulic conductivity K_{sat} and sorptivity (χ_o, a measure of the soil's tendency to imbibe water due to matric potential effects) are initially assumed to be homogeneous across the entire hillslope length ($L \gg \lambda$). We address the case where the soil is uniformly dry at the onset of a storm, where rainfall can be treated as having a uniform intensity (I) for the storm duration, and where overland flow mechanisms rather than water table responses dominate runoff production (i.e., arid rather than humid systems [cf. *Freeze*, 1972, 1974]). It is assumed that the microtopography is fixed and no erosion or accretion occurs. These assumptions are not generally met on real hillslopes. In the discussion, some of the implications of relaxing the assumption of homogeneity, specifically for the dynamically relevant cases where heterogeneities correlate with microtopographic features, are investigated. The range of plausible variability in soil hydraulic properties, roughness, macroporosity, vegetation growth and initial water content, however, means that addressing heterogeneity is an essentially unconstrained problem, lying beyond the scope of a single study, and its implications on upscaling the effects of microtopography are therefore discussed in general terms only.

[11] Two research questions were selected to guide the investigation of the simplified surface.

[12] 1. Does microtopography change the partitioning of rainfall into runoff and infiltration compared to a "background" state without microtopography (i.e., having A = 0)? and,

[13] 2. How do soil, slope, storm and microtopographic dimensions influence the degree of this change?

[14] As outlined above, this one-dimensional surface focuses the analysis on the two "end-member" cases A and D. Extensions of this approach by allowing for two-dimensionality and for hydroecogeomorphological feedbacks is outlined in the Discussion. Subscripts of "*m.t.*" for microtopography, and "*b.g.*" for the background reference case will be used to distinguish between background ($A = 0$) and microtopographically variable surfaces ($A > 0$) in the following description of the model.

3.1. Infiltration Prior to Ponding

[15] In dry soils, the water potential gradient imposed by the soil matrix dominates infiltration and gravitational effects may be neglected. As soils approaching saturation, matric potential effects are insignificant and infiltration is primarily driven by the gravitational potential or a unit gradient, resulting in essentially vertical flow [*Philip*, 1957]. Thus, the early stages of infiltration should respond to increases in infiltrating surface area (SA) regardless of its orientation, while the latter, vertical stages of infiltration would be dictated by the horizontal projection of SA. Thus, microtopography would increase the rate at which water is sorbed by the soil surface relative to a background state covering the same horizontal area. This behavior can be captured in the magnitude of the soil sorptivity [*Brutsaert*, 2005]. Where microtopographic variation is significant, the sorptivity measured at a point χ_o should underestimate the sorptivity at the hillslope scale ($\chi_{o_{m.t.}}$), unless a scaling factor is included to adjust for the increased surface area. We refer to this scaled value as the "effective sorptivity." Using Philip's solution for infiltration from hemispherical depressions [*Philip*, 1955, 1969, 1991] and a numerical model of infiltration based on Richards' equation over a sinusoidal depression, we verified that the effective sorptivity scaled in an almost one to one fashion with SA (Figure 3). Based on these results, it follows that

$$\chi_{o_{m.t.}} = \frac{SA_{m.t.}}{SA_{b.g.}} \chi_o. \qquad (1)$$

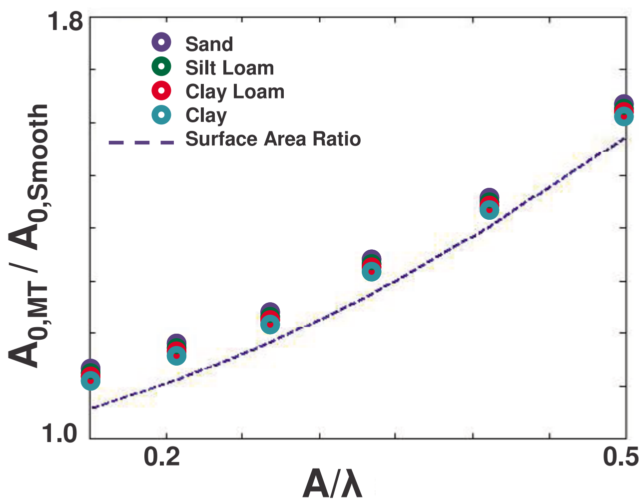

Figure 3. Effects of microtopography on infiltration dynamics based on a numerical solution to Richards' equation over a sinusoidal depression and for varying soil types. The effective sorptivity scales approximately 1:1 with the surface area ratio.

[16] The major implication of increased effective sorptivity is that the time to ponding (t_p) increases. A Smith and Parlange estimate of the time to ponding was adopted [*Parlange and Smith*, 1976]:

$$t_p = \frac{\chi_o^2}{2\, I\, K_{sat}\, \log(I/(I - K_{sat}))}, \tag{2}$$

where I is, as before, the rainfall intensity assumed to be uniform throughout the storm and across the hillslope, χ_o is the sorptivity and should be replaced by $\chi_{om.t.}$ in the presence of microtopography ($A > 0$), and K_{sat} is the saturated hydraulic conductivity. Note that where the A is small enough to approximate the scale of a soil pore, the continuum assumption behind this description of infiltration breaks down. Consequently, the surface area scaling should be treated as a macroscopic property and applied only for sufficiently large values of A.

3.2. Surface Storage: Case A

[17] Following ponding, runoff is initiated locally [*Horton*, 1945]. In the presence of microtopography, the initiation of non-local runoff is delayed until microtopographic depressions are filled. The volume of water that can be "sequestered" by these depressions is known as the surface store [*Allmaras et al.*, 1966; *de Lima et al.*, 1989; *Gayle and Skaggs*, 1978; *Hansen et al.*, 1999; *Linden and Vandoren*, 1986; *Mitchell and Jones*, 1976; *Mohamoud et al.*, 1990; *Planchon et al.*, 2002; *Van Oost et al.*, 2006; *Zobeck and Onstad*, 1987]. Some 40–70% of the time lag between rainfall and runoff initiation in experiments has been related to the peak size of the surface store [*Darboux and Huang*, 2005]. Strong positive linear correlations between amplitude and the peak storage [*Darboux et al.*, 2001; *Kamphorst et al.*, 2000; *Onstad*, 1984; *Zobeck and Onstad*, 1987], and strong negative linear correlations between slope angle and the peak storage [*Huang and Bradford*, 1990; *Kirkby et al.*, 2002] have been found, presumably as a direct geometric result.

[18] A toy model that accounts for the effects of the surface store can be constructed by computing a peak storage volume V_s and delaying the initiation of runoff until a time t_r when this storage is filled:

$$t_r = t_{p_{mt}} + \frac{V_s}{\int_{t_{p_{mt}}}^{t_r} (I - f)dt}, \tag{3}$$

where f is the infiltration rate which, following ponding, is given by

$$f = K_{sat} + \frac{1}{2}\chi_o\big(t - (t_p - t_{ca})\big)^{-1/2}, \tag{4}$$

where t_{ca} is the so-called compression time introduced to account for the shift in boundary condition from unsaturated to ponded infiltration [*Sivapalan and Milly*, 1989]. The choice of χ_o and t_p in equation (4) should reflect the surface condition (i.e., *b.g.* or *m.t.*).

3.3. Sheet Flow: Case D

[19] The flow over a microtopographic surface is complex and its complete description requires solution of (at least) the shallow water equations. A simple scale analysis of the shallow water mean momentum equation can provide insight into its behavior. If time scales as the microtopographic length scale over the bulk velocity ($2A/V$), and space as the microtopographic length-scale ($2A$), then

$$\frac{\partial}{\partial t}(Vh) + \frac{\partial}{\partial x}\left(V^2 h\right) + hg\frac{\partial h}{\partial x} = gh\left(S_o - S_f\right) \tag{5a}$$

$$\sim \left(\frac{V^2}{gh}\right)\left(\frac{h}{2A}\right) = S_o - S_f. \tag{5b}$$

Here S_o and S_f are the bed and energy grade-line (or friction) slopes, V is the depth-averaged velocity, h is the water depth, g the gravitational acceleration, and x is the direction along the hillslope. This analysis suggests that the Froude number $Fr^2 = \frac{V^2}{gh}$ and the inundation ratio $\frac{h}{2A}$ are the two control parameters for the shallow-water system, and are directly related to the local slope and roughness imposed by microtopography. The emergence of Fr as a control variable is expected for free surface flows, while the inundation ratio is the logical geometric variable.

[20] The most elementary treatment of roughness is via a Darcy-Weisbach friction factor given by $f_D = \frac{8\tau}{\rho V^2}$, where τ is the surface shear stress (viscous, turbulent, or their sum), and ρ is the water density. The dominant contribution to the shear is taken to be the pressure gradient term so that the friction factor may be decomposed as $\frac{8gh\sin\theta}{V^2} = \frac{8\sin\theta}{Fr^2}$, suggesting that a macroscopic parameterization of the roughness via a friction factor must implicitly depend upon Fr. Again, this is consistent with the importance of free surface effects (as parameterized by Fr) in contributing to the resistance to flow (parameterized by f_D) [*Smith et al.*, 2007].

[21] Experimentally, the friction factor that parameterizes resistance to a particular microtopographic arrangement

Table 1. Parameter Values for the Reference Case, Identification of the Model Runs in Which Their Effects Were Assessed, and the Range of Values Employed in These Model Runs

Parameter	Reference Value	Model Run	Range
A (m)	0.025	A	1 mm to 10 cm
λ (m)	0.4	A	10 cm to 2 m
I (m/s)	3.5×10^{-6}	B	10^{-6}–10^{-2} m/s
t_d (min)	30	B	30 min to 5 h
K_{sat} (m/s)	1×10^{-6}	C	10^{-10}–10^{-2} m/s
χ_o (m/s$^{1/2}$)	3.7×10^{-4}	C	10^{-6}–10^{-3} m/s$^{1/2}$
S_o (°)	2	D (results not shown)	10°
n (m$^{-1/3}$ s)	0.06 (2A)$^{1/6}$ (mt) 0.02 (smooth)	E (results not shown)	0.02

varies with inundation ratio [*Lawrence*, 1997, 2000]. The nature of this variation appears to be sensitive to specific geometric arrangements, making generalization of existing semi-empirical models challenging. As an alternative, we adopt the simple and conservative assumption that the resistance to the flow can be parameterized by relating the microtopography to the momentum roughness height (z_o) [*Chen*, 1991; *Katul et al.*, 2002], and assuming that z_o scales linearly with the depression height $2A$. We follow *Katul et al.* [2002] in linking the value of the friction factor to an estimate of Manning's friction factor (n) (or $f_D = 8n^2g/h^{1/3}$), such that $n \sim 0.06\ z_o^{1/6}$ (assuming turbulent flows). The n estimate is then used to parameterize a kinematic wave approximation to the overland flow. While this approach is undoubtedly an oversimplification, it provides a consistent and reproducible method. It offers a conservative estimate of the resistance in that this parameterization strictly applies to "deep flows" over microtopography, and probably underestimates the resistance where the inundation ratio is close to unity [*Katul et al.*, 2002]. We solved the flow equations following *Giráldez and Woolhiser* [1996] using the method of characteristics and accounting for the unsteady lateral inflow terms imposed by rainfall and infiltration:

$$\frac{\mathrm{dh}}{\mathrm{dt}} = \mathrm{I} - \mathrm{f} \tag{6a}$$

$$\frac{dx}{dt} = aK_r(h - 2A)^{a-1}, \tag{6b}$$

where I is the rainfall intensity, f, as before, is the infiltration rate (which is enhanced by microtopography), K_r is a kinematic resistance parameter defined in terms of the slope S_o and the roughness coefficient n, and is given as $K_r = \sqrt{S_o}/n$, and the exponent $a = 5/3$ for a turbulent overland flow regime (assumed when linking n to z_o) though a can be as large as 3 for a laminar flow regime. The modification to the celerity (6b) to depend on a reduced depth ensures that no flow occurs when $h < 2A$.

[22] The kinematic treatment assumes 1D flow and K_r inversely proportional to n. A finer level of detail could be obtained by considering a 2D formulation where the vertical dimension is explicitly incorporated and the differences in dynamics across the various water levels above the undulating surface are retained. Such a refinement would consider the effects of the undulating surface in depth (z) and x along the hillslope on the time-averaged longitudinal (U) and vertical (W) velocities via

$$\frac{\partial U}{\partial x} + \frac{\partial W}{\partial z} = 0 \tag{7a}$$

$$U\frac{\partial U}{\partial x} + W\frac{\partial U}{\partial z} \approx -\frac{1}{\rho}\frac{\partial P}{\partial x} - \frac{\partial \tau}{\partial z} - \frac{1}{2}C_d U^2, \tag{7b}$$

where C_d is the effective drag coefficient imposed by the microtopography on the flow (due to pressure and viscous effects), and τ is the sum of the turbulent and viscous stresses. The analysis can be simplified by assuming that the undulating surface primarily perturbs the mean pressure gradient $\partial P/\partial x$ (which is approximately out of phase with microtopography), in a vertically uniform manner, and that the mean longitudinal momentum balance responds by creating the advection terms. These advection terms modify the τ gradients given by $\tau = -(\nu_m + \nu_t)(\partial U/\partial z + \partial W/\partial x)$, where ν_t and ν_m are the turbulent and eddy-viscosity. Once the solution for $U(x, z)$ is derived using appropriate models for ν_t from this system as originally proposed by *Jackson and Hunt* [1975] (and also *Belcher and Hunt* [1998] and *Poggi et al.* [2007]), formal spatial averaging across the entire hill length can be employed to arrive at a bulk roughness parameter

$$f_D = \frac{1}{L}\int_0^L \frac{1}{h(x)}\int_0^{h(x)} \frac{8\tau(x,z)}{\rho U(x,z)^2}\,dz\,dx. \tag{8}$$

[23] The first order analysis with 1D flow did not indicate a strong sensitivity to the parameterization of the overland flow (see below), so this elaboration was not introduced for the numerical analysis presented here.

4. Numerical Analysis of the Idealized Case

[24] Even the simple toy model is dependent on a large number of parameters, precluding a factorial analysis across the entire parameter space. As an alternative, a reasonable reference condition was defined using realistic but fixed (unless otherwise specified) parameter values (Table 1). The reference soil properties correspond to clays with saturated hydraulic conductivities on the order of 10^{-6} m/s. The sorptivity of the soil χ_o was set to 3.7×10^{-4} m/s$^{1/2}$. Reference microtopography was set with A = 2.5 cm and wavelength λ of 40 cm. The reference rainfall was taken as an intense rainstorm with intensity 3.5×10^{-5} m/s and duration (t_d) of 30 min. For comparison, this approximates intensities associated with 2 year return periods in several dryland areas (e.g., northwestern Australia, or the northern Chihuahuan desert [*Bureau of Meteorology*, 2009; *Texas Department of Transportation*, 2009]).

[25] From this baseline, the soil (K_{sat}, χ_o), storm properties (I, t_d) properties, and microtopographic properties (A, λ) were varied. For each model run, the percentage of the rain partitioned into infiltration was calculated. This proportion was normalized by the partitioning to infiltration on a hillslope with A = 0 under otherwise identical conditions (i.e., the background state): it is this ratio that is reported. The model runs were repeated for slope angles of 2° and 10°;

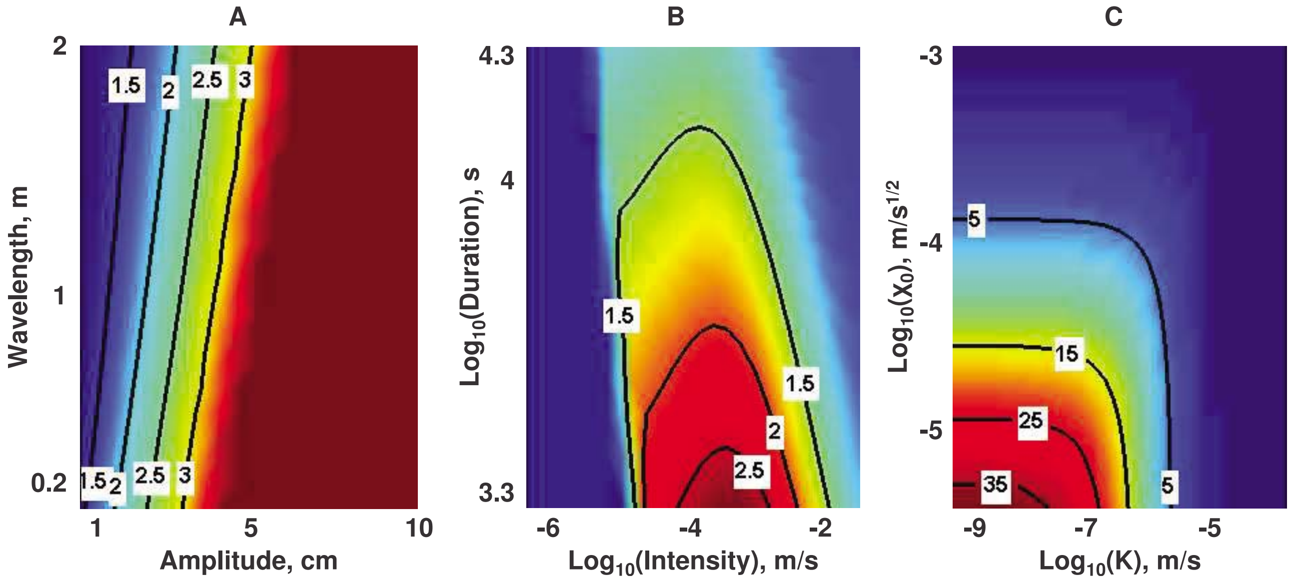

Figure 4. The proportional increase in infiltration per storm in the presence of microtopography (A > 0) relative to the background state (A = 0). Each plot represents variation in (a) microtopographic properties, (b) storm properties, and (c) soil properties about the background case (see Table 1).

and for a test case where the flow resistance parameter was held constant between the microtopographic and the background cases. The relative significance of the microtopography in increasing the time to ponding, the time to runoff generation (i.e., $t_r - t_p$), and the runoff regime (hydrographs) were also evaluated.

[26] Microtopography induced large increases in the proportion of incident rainfall that infiltrated, approximately doubling the percentage of rainfall that infiltrates in the reference case. The existence and magnitude of an increase in infiltration were sensitive to the soil properties, storm characteristics and microtopographic geometry. Similarly, the degree to which increased infiltration could be attributed to changes in time to ponding, the existence of the surface store or the change in hydraulic resistance varied with these factors.

4.1. Sensitivity to Microtopographic Dimensions

[27] For specified microtopographic amplitude, increasing the wavelength diminished the effects of microtopography. This decrease was subtle for low slope angles (Figure 4a), but became pronounced as the slope angles increased. Increasing the amplitude of the microtopography increased the proportion of infiltration markedly. The strong positive association of infiltration with increased microtopographic amplitude arose from the direct scaling between the amplitude and the time to ponding, the surface store and the resistance parameter (Figures 5a and 5b). The increase in time to ponding declined as the microtopographic wavelength increased, while the size of the surface store and the resistance parameter were near invariant with respect to wavelength (Figures 5a and 5b). The significant changes in partitioning associated with changes in the surface storage alone suggest that increases in the relative proportion of infiltrated water may still occur even where microtopographic variation is associated with the presence of impermeable obstacles (e.g., rocks, vegetation or debris).

4.2. Sensitivity to Storm Properties

[28] The sensitivity of the partitioning to storm properties peaked at intermediate rainfall intensities, and was greatest for storms of short duration. Where rainfall intensities were low, the time to ponding was not reached, or was of very short duration, such that discrepancies between background and microtopographic cases were minimal. Where rainfall intensities were high, the proportion of infiltration was low relative to the total rainfall volume for both microtopographic and background cases. Thus, an intermediate regime where rainfall intensities were 2–3 orders of magnitude greater than K_{sat} generated the most sensitive response (Figure 4b). Provided storm duration (t_d) was long enough to induce ponding on the background surface, the impact of microtopography was greatest for short storms.

4.3. Sensitivity to Soil Properties

[29] Microtopography caused the greatest increase in proportional infiltration where both the saturated hydraulic conductivity and the sorptivity were low. The increases in infiltration observed were entirely due to increased time to ponding relative to the background case as sorptivity declined. At medium-high sorptivities, time to ponding was not reached or occurred late in the storm, so both surfaces infiltrated most of the rainfall. At low sorptivities, the background surface ponded rapidly, causing a marked difference in runoff response compared to the microtopographic case.

4.4. Slope and Roughness Effects

[30] Two additional cases were considered. In the first of these cases, the results for a 2° slope as presented in Figures 4 and 5 were compared to the results for a 10° slope. Microtopography continued to exert an increase in infiltration relative to the background surfaces, but this increase declined (e.g., from a doubling of infiltration to a 50% increase for the reference case), primarily due to decreased

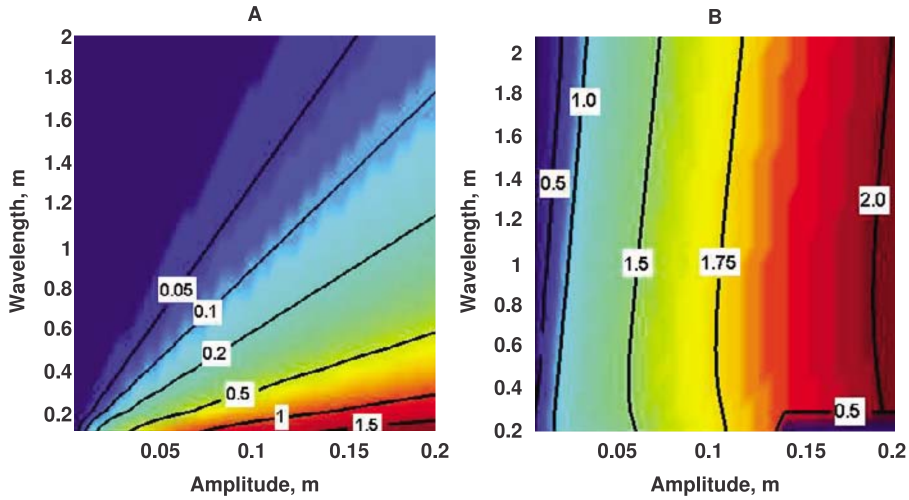

Figure 5. The increase in runoff initiation associated with the time to ponding and the storage time, both referenced against the time to ponding in the background case (see Table 1 for values). The proportional increases are rendered on a log scale to show their variation. (a) Time to ponding in the presence of microtopography relative to the background state and (b) Storage time associated with microtopography relative to the time to ponding. The runs were conducted with the usual reference properties and result in the change in total infiltration presented in Figure 4a.

storage volumes. The overall trends presented in Figures 4 and 5 remain representative despite the change in magnitude. The second comparison utilized a consistent resistance parameter for the background and microtopographically varying cases. This induced a small decrease in the effects of microtopography on infiltration and suggested that overall sensitivity to the resistance terms was not large in comparison to the infiltration effects.

5. Discussion

5.1. Toy Model Implications

[31] Based on the model results, microtopography may induce increases in the proportion of rainfall that infiltrates of 20 to 200% for short storms on shallow slopes. These increases are largest for larger microtopographic amplitude or where soils are heavy, degraded, or exhibit surface crusting and sealing (lower K_{sat} and χ_o). The results suggest that a suite of dimensionless numbers can be defined that control the sensitivity of the partitioning to microtopography:

$$\frac{I}{K_{sat}}, \frac{I\sqrt{t_d}}{\chi_o}, \frac{A}{\lambda}, \frac{L}{\lambda}, \frac{n_{m.t.}}{n_{b.g.}}$$

are all positively correlated with an increase in infiltration relative to the background surface. S_o, $\frac{t_d}{t_{pmt}}, \frac{t_d}{t_r}$ are negatively correlated to an increase in infiltration relative to a background surface. Microtopography increased infiltration and altered runoff thresholds. The relatively simple alteration of sorptivity and the large number of existing empirical models available for estimating the size of the surface store mean that it is not onerous to make first order amendments to existing hydrological models to account for these effects.

5.2. Theoretical Extensions

[32] As stated previously, the assumption of homogeneity and stationarity in the treatment above is not representative of "real world" conditions, where heterogeneity in soil properties is legion. Rather than attempt to address all possible sources of heterogeneity and their implications, we make an immediate distinction between heterogeneity induced by microtopography, and heterogeneity that may be superimposed on microtopographic landscapes. In the former case, the literature offers several interesting examples that provide opportunities to extend the simple treatment above, while the latter situation pertains primarily to upscaling results obtained to date.

5.2.1. Heterogeneity Induced by Microtopography

[33] Several sources of heterogeneity and non-stationarity are expected to correlate with microtopography. *Fox et al.* [1998] showed that microtopography was progressively eroded during a simulated rainfall event. Infiltration rates in the depressions were shown to be significantly less than those associated with mounds. The low infiltration rates were associated with the wash-in of fines and surface sealing. Drier soils may be expected at the peaks of microtopographic geometries and wetter conditions in the troughs. To explore the possible effects of such variation, we consider two prototypical cases where the infiltration rate is a function of the inundation. In one case, infiltration rates are highest on the mounds [*Bochet et al.*, 2000; *Dunne et al.*, 1991; *Fox et al.*, 1998]. We also present the alternative case, where infiltration rates are highest in the depressions, as might arise if clay soils result in increased cracking and macroporosity. Further extensions can be made where correlations develop during a storm e.g., due to surface sealing, or if A also becomes a function of time. Existing work developing infiltration theory in such cases provides an appropriate starting point [*Assouline and Mualem*, 1997, 2002]. For the temporally constant cases, a mathematical derivation is presented in the auxiliary material and only the key results are discussed here.[1] The results in

[1]Auxiliary materials are available in the HTML. doi:10.1029/2009WR008835.

the auxiliary material suggest that if correlations between microtopography and K_{sat} alter the spatially averaged value of K_{sat} relative to the background case, then the correlations may significantly dampen or amplify the effects of the microtopography depending on their phase relationship with microtopography. However, where the correlations leave the spatially averaged K_{sat} unaltered, they have essentially no impact on the partitioning. This result appears surprising when compared to Dunne et al.'s results, which showed strong sensitivity to correlations with K_{sat} and z. The distinction lies in the fact that in order to generate any runoff in this geometry, a depression must be fully inundated. For low slope conditions this results in essentially all the variability in K_{sat} being explored prior to runoff generation. Thus, the effective infiltration rate at the point of runoff generation is dictated by the spatial average of all values of K_{sat}, not a subset constrained by a comparatively shallow depth of flow as per Dunne et al.'s study. Consequently, the nonlinear coupling between runoff and infiltration is more dynamically variable and significant in that geometric arrangement.

5.2.2. Larger-Scale Heterogeneities and Upscaling

[34] Large-scale heterogeneities impose new length scales on hillslopes. If the effects of heterogeneity in isolation are anticipated to be on the same order of magnitude as the microtopographic effects, it may be necessary to move toward an explicit simulation approach [*Fiedler et al.*, 2002]. If, however, the impacts of imposed heterogeneities are sufficiently severe, then their effects may be dealt with by spatially decomposing the hillslope. Below the characteristic length scale on which the heterogeneities act, the microtopographic effects described here would dominate, while at longer length scales, the effects of the heterogeneities would become more pronounced. In combination with nonlinearities in the dynamics and length scales induced by the microtopographic variability itself (see below), this leads to the potential for highly scale-specific runoff and infiltration processes on hillslopes, as are known to arise in arid landscapes [*Kirkby et al.*, 2002; *Kirkby et al.*, 2005].

5.3. Challenges for Generalization

[35] When motivating this problem, two additional cases, B and C, were identified as posing challenges requiring new theoretical developments. The first development addresses the transition of the hillslope from a series of isolated depressions with independent and localized hydrologic balance to a connected network of basins contributing flow to their downstream neighbors and ultimately the channel. These fill-spill processes determine the formation of a surface flow network and have been identified as important in generating scale dependence in runoff [*Bergkamp*, 1998; *Joel et al.*, 2002; *Kirkby et al.*, 2002; *Puigdefabregas et al.*, 1999; *van De Giesen et al.*, 2000; *Wood et al.*, 1988] as well as introducing nonlinearity into runoff generation mechanisms [*Darboux et al.*, 2001; *Esteves and Lapetite*, 2003; *Kirkby*, 2001; *Lehmann et al.*, 2007; *Planchon et al.*, 2002; *Reaney et al.*, 2007; *van De Giesen et al.*, 2000]. Similar nonlinear scaling is familiar in the physics literature in studies of percolation or systems displaying criticality [*Bak et al.*, 1987; *Berkowitz and Ewing*, 1998; *Hammersley*, 1957; *Isichenko*, 1992], often yielding universal scaling properties [*Narayan and Fisher*, 1994]. Extending such approaches to account for infiltrating surfaces and flow forced by rainfall may provide useful and generalizable insights into surface connectivity.

[36] The second theoretical challenge addresses the description of the bulk flow properties of a partially submerged surface. Such flow is inherently complex, consisting of flow over and around submerged or emergent microtopographic features [*Lawrence*, 1997]. Macroscopically, microtopography segregates the flow into fast flowing "threads" moving at velocities 2–7 times greater than the mean velocity, and slow moving backwaters in which velocities approach zero [*Dunkerley*, 2003, 2004]. Up-scaling such variation, even empirically, is challenging [*Abrahams and Parsons*, 1990]. The development of theoretical approaches to study flows of this nature has been driven by approaches from the geomorphology, canopy flows, and gravel bed river communities [*Cooper et al.*, 2006; *Ferguson*, 2007; *Ferro*, 2003; *Hardy et al.*, 2007; *Katul et al.*, 2002; *Lacey and Roy*, 2007; *Lawrence*, 1997, 2000; *MacVicar and Roy*, 2007; *Marquis and Roy*, 2006]. All approaches highlight the importance of the relative degree of inundation of roughness elements. Similarity and scaling approaches based on the "inundation ratio" have proven at least as successful at describing the bulk flow properties as existing semi-empirical models [*Hey*, 1979; *Katul et al.*, 2002; *Lawrence*, 2000; *Leopold and Wolman*, 1960]. The description of the average properties of spatially variable flows remains challenging [*Canovaro et al.*, 2007], although new techniques are becoming available, such as acoustic "grazing angle sound propagation," which allows measurement of bulk roughness properties from the acoustic profile of the water surface [*Cooper et al.*, 2006]. The applicability of such techniques to overland flows is limited due to the shallow and variable depth of flow, meaning that drawing analogies from deeper, gravel lined channels, and scaled flume experiments remains the most promising way forward.

[37] At long timescales, feedbacks between vegetation, hydrology and geomorphology suggest the possibility of co-evolution of hillslope features. A prototypical example of the feedbacks between vegetation, microtopography and hydrology is in the role of vegetation in generating soil mounds [*Bochet et al.*, 2000; *Nash et al.*, 2003] with infiltration rates up to 2–8 times greater than surrounding soil [*Valentin et al.*, 1999]. *Saco et al.* [2007] demonstrated that feedbacks between biomass density, infiltration capacity and erodibility generated regular arrays of both vegetation and microtopographic mounds on arid hillslopes. Feedbacks between aeolian geomorphic features and vegetation are generate signatures of vegetation in landscape structures [*Baas and Nield*, 2007; *Nield and Baas*, 2008], while feedbacks between aeolian processes and hydrology have been shown to generate ring patterns in arid ecosystem vegetation [*Ravi et al.*, 2007]. The generation of microtopographic terracettes was explicitly considered by *Sanchez and Puigdefabregas* [1994] using cellular automata. Extending the focus of these studies from the generation of microtopography to the evolution of hydrological partitioning and ecological functioning is an area ripe for further exploration.

6. Conclusion

[38] Microtopographic variation was predicted to significantly alter hydrological partitioning where soils had low

permeability and were subject to intense rainstorms. The net effect of microtopography was to enhance the retention of rainfall in hillslope soils, which may represent a significant improvement in habitat and growing conditions for plants in the semiarid systems under consideration. The results suggest that under certain circumstances, ignoring microtopographic variation may lead to significant biases in prediction of hydrological partitioning of rainfall into infiltration and runoff. Modifications to classical hydrological theory through the use of an "effective sorptivity" and accounting for the peak surface store can be immediately applied. However, a more comprehensive theory that accounts for connectivity and the bulk representation of flow properties over variable terrain is needed, along with upscaling approaches to factor in other sources of variability in infiltration properties through space and time. Characterizing the properties of microtopography in real landscapes to allow its effective simulation and parsimonious description is a priority. Linking theoretical developments to the co-evolution of landscapes, specifically with regard to hydrological, geomorphological and ecological feedbacks, presents an exciting set of challenges for understanding and managing arid landscapes.

[39] **Acknowledgments.** S. Thompson acknowledges support from the General Sir John Monash Foundation and the National Science Foundation (NSF-EAR-06-28342 and NSF-EAR-06-35787). G. Katul acknowledges support from the National Science Foundation (NSF-EAR 06–35787, NSF-EAR-06-28432, and NSF-ATM-07-24088), the Binational Agricultural Research and Development (BARD, research grant IS3861-06). A.P. was supported by the U.S. National Science Foundation under grant EAR-0628342 and a collaboration grant from the U.S. Department of Agriculture, Agricultural Research Service, Temple, Texas. A.P. also gratefully acknowledges the support of the Landolt and Cie Chair "Innovative strategies for a sustainable future" at the École Polytechnique Fédérale de Lausanne, Lausanne, Switzerland.

References

Abrahams, A. D., and A. J. Parsons (1990), Determining the mean depth of overland-flow in field studies of flow hydraulics, *Water Resour. Res.*, *26*(3), 501–503.

Allmaras, R. R., R. E. Burwell, W. E. Larson, R. F. Holt, and W. W. Nelson (1966), Total porosity and random roughness of the interrow zone as influenced by tillage, *Conserv. Res. Rep. 7*, 22 pp., Agric. Resour. Serv., U.S. Dep. of Agric., Washington, D. C.

Assouline, S., and Y. Mualem (1997), Modeling the dynamics of seal formation and its effect on infiltration as related to soil and rainfall characteristics, *Water Resour. Res.*, *33*(7), 1527–1536, doi:10.1029/96WR02674.

Assouline, S., and Y. Mualem (2002), Infiltration during soil sealing: The effect of areal heterogeneity of soil hydraulic properties, *Water Resour. Res.*, *38*(12), 1286, doi:10.1029/2001WR001168.

Baas, A. C. W., and J. M. Nield (2007), Modelling vegetated dune landscapes, *Geophys. Res. Lett.*, *34*, L06405, doi:10.1029/2006GL029152.

Bak, P., C. Tang, and K. Wiesenfeld (1987), Self-organized criticality—An explanation of 1/F noise, *Phys. Rev. Lett.*, *59*(4), 381–384, doi:10.1103/PhysRevLett.59.381.

Belcher, S. E., and J. C. R. Hunt (1993), Turbulent shear-flow over slowly moving waves, *J. Fluid Mech.*, *251*, 109–148, doi:10.1017/S0022112093003350.

Belcher, S. E., and J. C. R. Hunt (1998), Turbulent flow over hills and waves, *Annu. Rev. Fluid Mech.*, *30*, 507–538, doi:10.1146/annurev.fluid.30.1.507.

Bergkamp, G. (1998), A hierarchical view of the interactions of runoff and infiltration with vegetation and microtopography in semiarid shrublands, *Catena*, *33*(3–4), 201–220, doi:10.1016/S0341-8162(98)00092-7.

Berkowitz, B., and R. P. Ewing (1998), Percolation theory and network modeling applications in soil physics, *Surv. Geophys.*, *19*(1), 23–72, doi:10.1023/A:1006590500229.

Bochet, E., J. Poesen, and J. L. Rubio (2000), Mound development as an interaction of individual plants with soil, water erosion and sedimentation processes on slopes, *Earth Surf. Processes Landforms*, *25*(8), 847–867, doi:10.1002/1096-9837(200008)25:8<847::AID-ESP103>3.0.CO;2-Q.

Brutsaert, W. (2005), *Hydrology: An Introduction*, pp. 307–361, Cambridge Univ. Press, New York.

Bureau of Meteorology (2009), *Intensity Frequency Duration Data for Karratha, Western Australia*, Melbourne, Victoria, Australia.

Burrough, P. A. (1983), Multiscale sources of spatial variation in soil. 1. The application of fractal concepts to nested levels of soil variation, *J. Soil Sci.*, *34*(3), 577–597, doi:10.1111/j.1365-2389.1983.tb01057.x.

Canovaro, F., E. Paris, and L. Solari (2007), Effects of macro-scale bed roughness geometry on flow resistance, *Water Resour. Res.*, *43*, W10414, doi:10.1029/2006WR005727.

Chen, C. L. (1991), Unified theory on power-laws for flow resistance, *J. Hydraul. Eng.*, *117*, 371–389, doi:10.1061/(ASCE)0733-9429(1991)117:3(371).

Cooper, J. R., S. J. Tait, and K. V. Horoshenkov (2006), Determining hydraulic resistance in gravel-bed rivers from the dynamics of their water surfaces, *Earth Surf. Processes Landforms*, *31*(14), 1839–1848, doi:10.1002/esp.1447.

Costa, M. F. M. (2004), Application of image processing to the characterisation of nanostructures, *Rev. Adv. Mater. Sci.*, *6*(1), 12–20.

Darboux, F., and C. H. Huang (2005), Does soil surface roughness increase or decrease water and particle transfers?, *Soil Sci. Soc. Am. J.*, *69*(3), 748–756, doi:10.2136/sssaj2003.0311.

Darboux, F., P. Davy, C. Gascuel-Odoux, and C. Huang (2001), Evolution of soil surface roughness and flowpath connectivity in overland flow experiments, *Catena*, *46*(2–3), 125–139.

de Lima, J., L. Eppink, and W. H. Vandermolen (1989), A kinematic overland-flow model to determine depression storage of tilled surfaces, *Soil Tillage Res.*, *15*(1–2), 65–78, doi:10.1016/0167-1987(89)90064-0.

Texas Department of Transportation (2009), Hydraulic design manual: The rational method, Austin, Tex.

Descroix, L., D. Viramontes, J. Estrada, J. L. G. Barrios, and J. Asseline (2007), Investigating the spatial and temporal boundaries of Hortonian and Hewlettian runoff in northern Mexico, *J. Hydrol.*, *346*(3–4), 144–158, doi:10.1016/j.jhydrol.2007.09.009.

Dunkerley, D. (2003), Determining friction coefficients for inter-rill flows: The significance of flow filaments and backwater effects, *Earth Surf. Processes Landforms*, *28*(5), 475–491, doi:10.1002/esp.453.

Dunkerley, D. (2004), Flow threads in surface run-off: Implications for the assessment of flow properties and friction coefficients in soil erosion and hydraulics investigations, *Earth Surf. Processes Landforms*, *29*(8), 1011–1026, doi:10.1002/esp.1086.

Dunne, T., W. H. Zhang, and B. F. Aubry (1991), Effects of rainfall, vegetation, and microtopography on infiltration and runoff, *Water Resour. Res.*, *27*(9), 2271–2285, doi:10.1029/91WR01585.

Esteves, M., and J. M. Lapetite (2003), A multi-scale approach of runoff generation in a Sahelian gully catchment: A case study in Niger, *Catena*, *50*(2–4), 255–271, doi:10.1016/S0341-8162(02)00136-4.

Esteves, M., X. Faucher, S. Galle, and M. Vauclin (2000), Overland flow and infiltration modelling for small plots during unsteady rain: Numerical results versus observed values, *J. Hydrol.*, *228*(3–4), 265–282, doi:10.1016/S0022-1694(00)00155-4.

Ferguson, R. (2007), Flow resistance equations for gravel- and boulder-bed streams, *Water Resour. Res.*, *43*, W05427, doi:10.1029/2006WR005422.

Ferro, V. (2003), Flow resistance in gravel-bed channels with large-scale roughness, *Earth Surf. Processes Landforms*, *28*(12), 1325–1339, doi:10.1002/esp.589.

Fiedler, F. R., and J. A. Ramirez (2000), A numerical method for simulating discontinuous shallow flow over an infiltrating surface, *Int. J. Numer. Methods Fluids*, *32*(2), 219–239, doi:10.1002/(SICI)1097-0363(20000130)32:2<219::AID-FLD936>3.0.CO;2-J.

Fiedler, F. R., G. W. Frasier, J. A. Ramirez, and L. R. Ahuja (2002), Hydrologic response of grasslands: Effects of grazing, interactive infiltration, and scale, *J. Hydrol. Eng.*, *7*(4), 293–301, doi:10.1061/(ASCE)1084-0699(2002)7:4(293).

Finnigan, J. J., and S. E. Belcher (2004), Flow over a hill covered with a plant canopy, *Q. J. R. Meteorol. Soc.*, *130*, 1–29, doi:10.1256/qj.02.177.

Fox, D. M., Y. Le Bissonnais, and P. Quetin (1998), The implications of spatial variability in surface seal hydraulic resistance for infiltration in a mound and depression microtopography, *Catena*, *32*(2), 101–114, doi:10.1016/S0341-8162(98)00043-5.

Freeze, R. A. (1972), Role of subsurface flow in generating surface runoff: 2. Upstream source areas, *Water Resour. Res.*, *8*(5), 1272–1283, doi:10.1029/WR008i005p01272.

Freeze, R. A. (1974), Streamflow generation, *Rev. Geophys.*, *12*(4), 627–647, doi:10.1029/RG012i004p00627.

Gayle, G. A., and R. W. Skaggs (1978), Surface storage on bedded cultivated lands, *Trans. ASAE*, *21*(1), 101–104.

Giráldez, J. V., and D. A. Woolhiser (1996), Analytical integration of the kinematic equation for runoff on a plane under constant rainfall rate and Smith and Parlange infiltration, *Water Resour. Res.*, *32*(11), 3385–3389, doi:10.1029/96WR02106.

Hale, M. S., and J. G. Mitchell (2002), Effects of particle size, flow velocity, and cell surface microtopography on the motion of submicrometer particles over diatoms, *Nano Lett.*, *2*(6), 657–663, doi:10.1021/nl025557m.

Hammersley, J. M. (1957), Percolation processes: Lower bounds for the critical probability, *Ann. Math. Stat.*, *28*(3), 790–795, doi:10.1214/aoms/1177706894.

Hansen, B., P. Schjonning, and E. Sibbesen (1999), Roughness indices for estimation of depression storage capacity of tilled soil surfaces, *Soil Tillage Res.*, *52*(1–2), 103–111, doi:10.1016/S0167-1987(99)00061-6.

Hardy, R. J., S. N. Lane, R. I. Ferguson, and D. R. Parsons (2007), Emergence of coherent flow structures over a gravel surface: A numerical experiment, *Water Resour. Res.*, *43*, W03422, doi:10.1029/2006WR004936.

Helming, K., M. J. M. Romkens, and S. N. Prasad (1998), Surface roughness related processes of runoff and soil loss: A flume study, *Soil Sci. Soc. Am. J.*, *62*(1), 243–250.

Hey, R. D. (1979), Flow resistance in gravel-bed rivers, *J. Hydraul. Div. Am. Soc. Civ. Eng.*, *105*(4), 365–379.

Horton, R. E. (1945), Erosional development of streams and their drainage basins: Hydrophysical approach to quantitative morphology, *Geol. Soc. Am. Bull.*, *56*(3), 275–370, doi:10.1130/0016-7606(1945)56[275:EDOSAT]2.0.CO;2.

Huang, C., and J. M. Bradford (1990), Depressional storage for Markov-Gaussian surfaces, *Water Resour. Res.*, *26*(9), 2235–2242.

Isichenko, M. B. (1992), Percolation, statistical topography, and transport in random-media, *Rev. Mod. Phys.*, *64*(4), 961–1043, doi:10.1103/RevModPhys.64.961.

Jackson, P. S., and J. C. R. Hunt (1975), Turbulent wind flow over a low hill, *Q. J. R. Meteorol. Soc.*, *101*(430), 929–955, doi:10.1002/qj.49710143015.

Joel, A., I. Messing, O. Seguel, and M. Casanova (2002), Measurement of surface water runoff from plots of two different sizes, *Hydrol. Processes*, *16*(7), 1467–1478, doi:10.1002/hyp.356.

Johnson, C. B., J. V. Mannering, and W. C. Moldenhauer (1979), Influence of surface-roughness and clod size and stability on soil and water losses, *Soil Sci. Soc. Am. J.*, *43*(4), 772–777.

Kamphorst, E. C., V. Jetten, J. Guerif, J. Pitkanen, B. V. Iversen, J. T. Douglas, and A. Paz (2000), Predicting depressional storage from soil surface roughness, *Soil Sci. Soc. Am. J.*, *64*(5), 1749–1758.

Katul, G., P. Wiberg, J. Albertson, and G. Hornberger (2002), A mixing layer theory for flow resistance in shallow streams, *Water Resour. Res.*, *38*(11), 1250, doi:10.1029/2001WR000817.

Kirkby, M. (2001), Modelling the interactions between soil surface properties and water erosion, *Catena*, *46*(2–3), 89–102.

Kirkby, M. J., and R. J. Chorley (1967), Throughflow, overland flow and erosion, *Bull. Int. Assoc. Sci. Hydrol.*, *12*(3), 5–21, doi:10.1080/02626666709493533.

Kirkby, M., L. Bracken, and S. Reaney (2002), The influence of land use, soils and topography on the delivery of hillslope runoff to channels in SE Spain, *Earth Surf. Processes Landforms*, *27*(13), 1459–1473, doi:10.1002/esp.441.

Kirkby, M. J., L. J. Bracken, and J. Shannon (2005), The influence of rainfall distribution and morphological factors on runoff delivery from dryland catchments in SE Spain, *Catena*, *62*(2–3), 136–156, doi:10.1016/j.catena.2005.05.002.

Lacey, R. W. J., and A. G. Roy (2007), A comparative study of the turbulent flow field with and without a pebble cluster in a gravel bed river, *Water Resour. Res.*, *43*, W05502, doi:10.1029/2006WR005027.

Lawrence, D. S. L. (1997), Macroscale surface roughness and frictional resistance in overland flow, *Earth Surf. Processes Landforms*, *22*(4), 365–382, doi:10.1002/(SICI)1096-9837(199704)22:4<365::AID-ESP693>3.0.CO;2-6.

Lawrence, D. S. L. (2000), Hydraulic resistance in overland flow during partial and marginal surface inundation: Experimental observations and modeling, *Water Resour. Res.*, *36*(8), 2381–2393, doi:10.1029/2000WR900095.

Lehmann, P., C. Hinz, G. McGrath, H. J. Tromp-van Meerveld, and J. J. McDonnell (2007), Rainfall threshold for hillslope outflow: An emergent property of flow pathway connectivity, *Hydrol. Earth Syst. Sci.*, *11*(2), 1047–1063, doi:10.5194/hess-11-1047-2007.

Leopold, L. B., and M. G. Wolman (1960), River meanders, *Geol. Soc. Am. Bull.*, *71*(6), 769–793, doi:10.1130/0016-7606(1960)71[769:RM]2.0.CO;2.

Linden, D. R., and D. M. Vandoren (1986), Parameters for characterizing tillage-induced soil surface-roughness, *Soil Sci. Soc. Am. J.*, *50*(6), 1560–1565.

Lloyd, W. R. (2003), Microtopography for ductile fracture process characterization part 1: Theory and methodology, *Eng. Fract. Mech.*, *70*(3–4), 387–401, doi:10.1016/S0013-7944(02)00126-1.

MacVicar, B. J., and A. G. Roy (2007), Hydrodynamics of a forced riffle pool in a gravel bed river: 2. Scale and structure of coherent turbulent events, *Water Resour. Res.*, *43*, W12402, doi:10.1029/2006WR005274.

Marquis, G. A., and A. G. Roy (2006), Effect of flow depth and velocity on the scales of macroturbulent structures in gravel-bed rivers, *Geophys. Res. Lett.*, *33*, L24406, doi:10.1029/2006GL028420.

Mitchell, J. K., and A. J. Jones (1976), Micro-relief surface depression storage: Analysis of models to describe the depth-storage function, *Water Resour. Bull.*, *12*(6), 1205–1223.

Mohamoud, Y. M., L. K. Ewing, and C. W. Boast (1990), Small plot hydrology. 1. Rainfall infiltration and depression-storage determination, *Trans. ASAE*, *33*(4), 1121–1131.

Narayan, O., and D. S. Fisher (1994), Nonlinear fluid-flow in random media—Critical phenomena near threshold, *Phys. Rev. B*, *49*(14), 9469–9502, doi:10.1103/PhysRevB.49.9469.

Nash, M. S., E. Jackson, and W. G. Whitford (2003), Soil microtopography on grazing gradients in Chihuahuan desert grasslands, *J. Arid Environ.*, *55*(1), 181–192, doi:10.1016/S0140-1963(02)00251-3.

Nield, J. M., and A. C. W. Baas (2008), Investigating parabolic and nebkha dune formation using a cellular automaton modelling approach, *Earth Surf. Processes Landforms*, *33*(5), 724–740, doi:10.1002/esp.1571.

Noy-Meir, I. (1979), Structure and function of desert ecosystems, *Isr. J. Bot.*, *28*(1), 1–19.

Onstad, C. A. (1984), Depressional storage on tilled soil surfaces, *Trans. ASAE*, *27*(3), 729–732.

Pachepsky, Y. A., and J. C. Ritchie (1998), Seasonal changes in fractal landscape surface roughness estimated from airborne laser altimetry data, *Int. J. Remote Sens.*, *19*(13), 2509–2516, doi:10.1080/014311698214596.

Pachepsky, Y. A., J. C. Ritchie, and D. Gimenez (1997), Fractal modeling of airborne laser altimetry data, *Remote Sens. Environ.*, *61*(1), 150–161, doi:10.1016/S0034-4257(96)00249-0.

Pardini, G., and F. Gallart (1998), A combination of laser technology and fractals to analyse soil surface roughness, *Eur. J. Soil Sci.*, *49*(2), 197–202, doi:10.1046/j.1365-2389.1998.00149.x.

Parlange, J. Y., and R. E. Smith (1976), Ponding time for variable infiltration rates, *Can. J. Soil Sci.*, *56*, 121–123, doi:10.4141/cjss76-019.

Patton, E., and G. G. Katul (2009), Turbulent pressure and velocity perturbations induced by gentle hills covered with sparse and dense canopies, *Boundary Layer Meteorol.*, *133*, 189–217, doi:10.1007/s10546-009-9427-x.

Perfect, E., and B. D. Kay (1995), Applications of fractals in soil and tillage research: A review, *Soil Tillage Res.*, *36*(1–2), 1–20, doi:10.1016/0167-1987(96)81397-3.

Philip, J. R. (1955), Numerical solution of equations of the diffusion type with diffusivity concentration-dependent, *Trans. Faraday Soc.*, *51*(7), 885–892, doi:10.1039/tf9555100885.

Philip, J. R. (1957), The theory of infiltration: 1. The infiltration equation and its solution, *Soil Sci.*, *83*, 345–357.

Philip, J. R. (1969), Early stages of infiltration in two-dimensional and three-dimensional systems, *Aust. J. Soil Res.*, *7*(3), 213–221, doi:10.1071/SR9690213.

Philip, J. R. (1991), Infiltration and downslope unsaturated flows in concave and convex topographies, *Water Resour. Res.*, *27*(6), 1041–1048, doi:10.1029/91WR00129.

Planchon, O., M. Esteves, N. Silvera, and J. M. Lapetite (2002), Microrelief induced by tillage: Measurement and modelling of surface storage capacity, *Catena*, *46*(2–3), 141–157, doi:10.1016/S0341-8162(01)00163-1.

Poggi, D., G. G. Katul, J. D. Albertson, and L. Ridolfi (2007), An experimental investigation of turbulent flows over a hilly surface, *Phys. Fluids*, *19*(3), 036601, doi:10.1063/1.2565528.

Poggi, D., G. Katul, J. J. Finnigan, and S. E. Belcher (2008), Analytical models for the mean flow inside dense canopies on gentle hilly terrain, *Q. J. R. Meteorol. Soc.*, *134*, 1095–1112, doi:10.1002/qj.276.

Puigdefabregas, J., A. Sole, L. Gutierrez, G. del Barrio, and M. Boer (1999), Scales and processes of water and sediment redistribution in drylands: Results from the Rambla Honda field site in southeast Spain, *Earth Sci. Rev.*, *48*(1–2), 39–70, doi:10.1016/S0012-8252(99)00046-X.

Ravi, S., P. D'Odorico, and G. S. Okin (2007), Hydrologic and aeolian controls on vegetation patterns in arid landscapes, *Geophys. Res. Lett.*, *34*, L24S23, doi:10.1029/2007GL031023.

Reaney, S. M., L. J. Bracken, and M. J. Kirkby (2007), Use of the connectivity of runoff model (CRUM) to investigate the influence of storm characteristics on runoff generation and connectivity in semi-arid areas, *Hydrol. Processes*, *21*(7), 894–906, doi:10.1002/hyp.6281.

Saco, P. M., G. R. Willgoose, and G. R. Hancock (2007), Eco-geomorphology of banded vegetation patterns in arid and semi-arid regions, *Hydrol. Earth Syst. Sci.*, *11*, 1717–1730, doi:10.5194/hess-11-1717-2007.

Sanchez, G., and J. Puigdefabregas (1994), Interactions of plant-growth and sediment movement on slopes in a semiarid environment, *Geomorphology*, *9*(3), 243–260, doi:10.1016/0169-555X(94)90066-3.

Semler, E. J., C. S. Ranucci, and P. V. Moghe (2006), Tissue assembly guided via substrate biophysics: Applications to hepatocellular engineering, *Tissue Eng.*, *102*, 1–46.

Sivapalan, M., and P. C. D. Milly (1989), On the relationship between the time condensation approximation and the flux concentration relation, *J. Hydrol.*, *105*(3–4), 357–367, doi:10.1016/0022-1694(89)90113-3.

Smith, M. W., N. J. Cox, and L. J. Bracken (2007), Applying flow resistance equations to overland flows, *Prog. Phys. Geogr.*, *31*(4), 363–387, doi:10.1177/0309133307081289.

Steichen, J. M. (1984), Infiltration and random roughness of a tilled and untilled claypan soil, *Soil Tillage Res.*, *4*(3), 251–262, doi:10.1016/0167-1987(84)90024-2.

Tayfur, G., M. L. Kavvas, R. S. Govindaraju, and D. E. Storm (1993), Applicability of St-Venant equations for 2-dimensional overland flows over rough infiltrating surfaces, *J. Hydraul. Eng.*, *119*(1), 51–63, doi:10.1061/(ASCE)0733-9429(1993)119:1(51).

Valentin, C., J. M. d'Herbes, and J. Poesen (1999), Soil and water components of banded vegetation patterns, *Catena*, *37*(1–2), 1–24, doi:10.1016/S0341-8162(99)00053-3.

van De Giesen, N. C., T. J. Stomph, and N. de Ridder (2000), Scale effects of Hortonian overland flow and rainfall-runoff dynamics in a West African catena landscape, *Hydrol. Processes*, *14*(1), 165–175, doi:10.1002/(SICI)1099-1085(200001)14:1<165::AID-HYP920>3.0.CO;2-1.

Vanenckevort, W. J. P. (1984), Surface microtopography of aqueous-solution grown crystals, *Prog. Cryst. Growth Charact. Mater.*, *9*(1–2), 1–50.

Van Oost, K., G. Govers, S. de Alba, and T. A. Quine (2006), Tillage erosion: A review of controlling factors and implications for soil quality, *Prog. Phys. Geogr.*, *30*(4), 443–466, doi:10.1191/0309133306pp487ra.

Vazquez, E. V., J. G. V. Miranda, and A. P. Gonzalez (2005), Characterizing anisotropy and heterogeneity of soil surface microtopography using fractal models, *Ecol. Modell.*, *182*(3–4), 337–353, doi:10.1016/j.ecolmodel.2004.04.012.

Wood, E. F., M. Sivapalan, K. Beven, and L. Band (1988), Effects of spatial variability and scale with implications to hydrologic modeling, *J. Hydrol.*, *102*(1–4), 29–47, doi:10.1016/0022-1694(88)90090-X.

Zobeck, T. M., and C. A. Onstad (1987), Tillage and rainfall effects on random roughness—A review, *Soil Tillage Res.*, *9*(1), 1–20, doi:10.1016/0167-1987(87)90047-X.

G. G. Katul and S. E. Thompson, Nicholas School of the Environment, Duke University, Durham, NC 27701, USA. (set8@duke.edu)

A. Porporato, Pratt School of Engineering, Duke University, Durham, NC 27701, USA.